

## High-Fat Diet Causes Lipotoxicity Responses in Cumulus–Oocyte Complexes and Decreased Fertilization Rates

Linda Lin-Yan Wu, Kylie R. Dunning, Xing Yang, Darryl L. Russell, Michelle Lane, Robert J. Norman, and Rebecca L. Robker

School of Pediatrics and Reproductive Health (L.L.-Y.W., K.R.D., X.Y., D.L.R., M.L., R.J.N., R.L.R.), Robinson Institute, University of Adelaide, Adelaide, South Australia 5005, Australia; Reproductive Medical Centre (X.Y.), Sixth Affiliated Hospital of Sun Yat-sen University, Guangzhou, China 510275; and Repromed (M.L.), Dulwich, South Australia 5065, Australia

In obesity, accumulation of lipid in nonadipose tissues, or lipotoxicity, is associated with endoplasmic reticulum (ER) stress, mitochondrial dysfunction, and ultimately apoptosis. We have previously shown that obese women have increased triglycerides in follicular fluid; thus, the present study examined whether high-fat diet–induced obesity causes lipotoxicity in granulosa cells and the cumulus–oocyte complex (COC). Oocytes of mice fed a high-fat diet had dramatically increased lipid content and reduced mitochondrial membrane potential compared to those of mice fed a control diet. COCs from mice fed a high-fat diet had increased expression of ER stress marker genes ATF4 and GRP78. Apoptosis was increased in granulosa and cumulus cells of mice fed a high-fat diet. Mice fed a high-fat diet also exhibited increased anovulation and decreased *in vivo* fertilization rates. Thus, lipid accumulation, ER stress, mitochondrial dysfunction, and apoptosis are markedly increased in ovarian cells of mice fed a high-fat diet. ER stress markers were also analyzed in granulosa cells and follicular fluid from women with varying body mass indices (BMI). ATF4 was increased in granulosa cells and  $[Ca^{2+}]$  in follicular fluid from obese women compared to nonobese women. These results indicate that lipotoxicity may be occurring in ovarian cells of obese women and may contribute to the reduced pregnancy rates observed in response to obesity. (*Endocrinology* 151: 5438–5445, 2010)

Obese women have a higher prevalence of infertility than their lean counterparts. Obesity is a risk factor for anovulation (1, 2), including in response to gonadotropin treatment (3). Further, even in women who are cycling regularly, obesity is associated with increased time-to-pregnancy (4–6) and decreased chance of natural pregnancy (7, 8).

During obesity or periods of overnutrition, lipid accumulates in nonadipose tissues, notably skeletal muscle, liver, heart, and pancreas (9) due to cellular uptake of exogenous fatty acids, triglycerides, and cholesterol as well as *de novo* lipogenesis in response to elevated glucose. The accumulation of intracellular lipid leads to high levels of free fatty acids that are subject to oxidative damage and the formation of cytotoxic and highly reactive lipid per-

oxides, which ultimately are detrimental to intracellular organelles, particularly the endoplasmic reticulum (ER) and mitochondria (10–12). Exposure of the ER to high levels of free fatty acids and lipid peroxides causes structural alterations that perturb ER function (13, 14) and lead to accumulation of unfolded proteins and calcium release. The aggregation of unfolded proteins activates a compensatory reaction, termed the unfolded protein response (UPR), a coordinated response that includes cell cycle arrest, transient attenuation of global protein synthesis and activation of ER-associated protein degradation, and induction of chaperone proteins and folding catalysts (15, 16). Failure of the UPR to reestablish ER homeostasis can lead to apoptosis (15, 16). When mitochondria are exposed to high levels of free fatty acids, these

ISSN Print 0013-7227 ISSN Online 1945-7170  
Printed in U.S.A.

Copyright © 2010 by The Endocrine Society  
doi: 10.1210/en.2010-0551 Received May 14, 2010. Accepted August 18, 2010.  
First Published Online September 22, 2010

Abbreviations: BMI, Body mass index; COC, cumulus–oocyte complex; eCG, equine chorionic gonadotropin; ER, endoplasmic reticulum; hCG, human chorionic gonadotropin; MMP, mitochondrial membrane potential; UPR, unfolded protein response.

can become oxidized by mitochondrial reactive oxygen species, forming lipid peroxides that damage essential proteins and uncouple mitochondrial function (17). This results in mitochondrial damage, which can cause further accumulation of lipids that cannot be catabolized, disrupted cellular homeostasis, and ultimately apoptosis (10, 18).

Thus, in  $\beta$ -cells, hepatocytes, and Chinese hamster ovary (CHO) and H9c2 cardiomyoblasts cell lines, high levels of fatty acids lead to oxidative stress, ER stress, and mitochondrial dysfunction that initiates a cascade of lipid-induced programmed cell-death, termed lipotoxicity (14, 19). Further, ER stress and lipotoxicity have been demonstrated in liver and brain from both diet-induced and genetic (ob/ob) mouse models of obesity (20, 21).

The cellular mechanisms by which obesity causes decreased conception rates are not known. Based on extensive evidence of obesity-induced lipotoxicity in other cells, we hypothesized that obesity results in the activation of lipotoxicity pathways in the ovary. Thus, this study sought to determine whether lipid accumulation, ER stress, mitochondrial dysfunction, and apoptosis occur in ovarian cells and the oocyte in response to a high-fat diet.

## Materials and Methods

### Animals

All animal experiments were approved by the University of Adelaide's Animal Ethics Committee and were conducted in accordance with the Australian Code of Practice for the Care and Use of Animals for Scientific Purposes. Female CBA mice were obtained from Laboratory Animal Services (South Australia) at 6 weeks of age and maintained on a 12-h light, 12-h dark cycle with rodent chow and water provided *ad libitum*. Mice were fed either a high-fat diet containing 22% fat (0.15% cholesterol), 19% protein, and 49.5% carbohydrate (SF00–219, Specialty Feeds) or a matched control diet containing 6% fat, 19% protein, and 64.7% carbohydrate (SF04-057, Specialty Feeds), as in our previous studies (22), for 4 wk. At the commencement of the dietary regimen all mice were of similar age and weight and all subsequent experiments were conducted with both groups simultaneously. Male CBA mice were maintained on standard rodent chow, were 10 to 16 wk old at mating, and were proven fertile.

To demonstrate the effects of the high-fat diet, one cohort of female mice was fasted overnight, weighed, and serum samples obtained for analysis of insulin, glucose, cholesterol, triglycerides, and free fatty acids. Mice fed high-fat diet had greater body weight compared with those fed control diet; the mean weight increase was 2 g or 11% of body weight (Supplemental Table 1 published on The Endocrine Society's Journals Online web site at <http://endo.endojournals.org/>). The high-fat diet also increased serum glucose and cholesterol levels (Supplemental Table 1).

### Isolation of mouse cumulus–oocyte complexes (COCs)

Immature, unexpanded COCs were collected by puncturing antral follicles of ovaries isolated 48 h after i.p. injection of 5 I.U. per 12 g body weight of equine chorionic gonadotropin (eCG,

Professional Compounding Centre of Australia) and mature, expanded COCs were obtained from oviducts by blunt dissection following 44 h eCG and 13 h post i.p. administration of 5 I.U. per 12 g body weight human chorionic gonadotropin (hCG/Pregnyl, Organon). COCs were collected in HEPES-buffered  $\alpha$  MEM (Invitrogen) supplemented with 5% (vol/vol) fetal calf serum. Media containing granulosa cells released during puncturing of follicles was centrifuged at 1500 rpm and cell pellets retained for RNA or DNA analyses.

### Lipid droplet staining and quantification

COCs were fixed in 4% paraformaldehyde/PBS for 4 h, washed in PBS, and transferred to 1  $\mu$ g/ml of the neutral lipid stain BODIPY 493/503 (Invitrogen) in PBS for 1 h in the dark at room temperature. After staining, COCs were washed in PBS for 5 min and mounted on coverslips in 3  $\mu$ l PBS. To prevent COCs sticking to pipettes 1 mg/ml polyvinylpyrrolidone was included in each solution. Images of each COC were captured by Leica SP5 spectral scanning confocal microscope using identical magnification and gain settings throughout experiments. Using Analysis Pro software (Olympus), a rectangle was placed across the COC image or a square of fixed size placed at the oocyte center (see Figure 1). The average fluorescence intensity in each pixel column across the box was reported. The mean  $\pm$  SEM was calculated for all COCs/oocytes and represented graphically as intensity of fluorescence over pixel widths. Total lipid content was determined as the sum total of fluorescence in the boxed area.

### RNA isolation and real-time RT-PCR

Total RNA was isolated from COCs or granulosa cells using RNeasy Micro Kit (Qiagen) as per manufacturer's instructions. RNA concentration and purity were quantified using a Nanodrop ND-1000 Spectrophotometer (Biolab) before reverse transcribing 600 ng RNA using random primers (Roche) and Superscript III Reverse Transcriptase (Invitrogen) according to the manufacturer's instructions. Ribosomal protein L19 (RPL19) was used as a validated internal control for every sample. All primers were Quantitect Primer Assays (Qiagen) and shown to have comparable amplification efficiency against the internal control. Real-time PCR was performed in triplicate using SYBR<sup>®</sup> Green PCR Master Mix (Applied Biosystems) and a Rotor-Gene 6000 (Corbett) real-time rotary analyzer. Real-time RT-PCR data were analyzed using the  $\Delta\Delta$ CT method and expressed as the fold change relative to a calibrator sample which was included in each run.

### Analysis of inner mitochondrial membrane potential

Denuded oocytes were incubated with the inner membrane dye JC-1 (5,5',6,6'-tetrachloro-1,1',3,3', tetraethylbenzimidazolylcarbocyanine iodide, Invitrogen) at 1.5 mM for 15 min at 37 C in the dark. Oocytes were then imaged immediately in both green and red fluorescence channel using Leica SP5 spectral scanning confocal microscope. Fluorescence intensity in each oocyte was quantified as in the fluorescent lipid quantification assay above.

### DNA ladder assay

Granulosa cells were resuspended in 400  $\mu$ l lysis buffer [10 mM Tris (pH 8.0), 100 mM NaCl, 25 mM EDTA, 0.5% SDS].

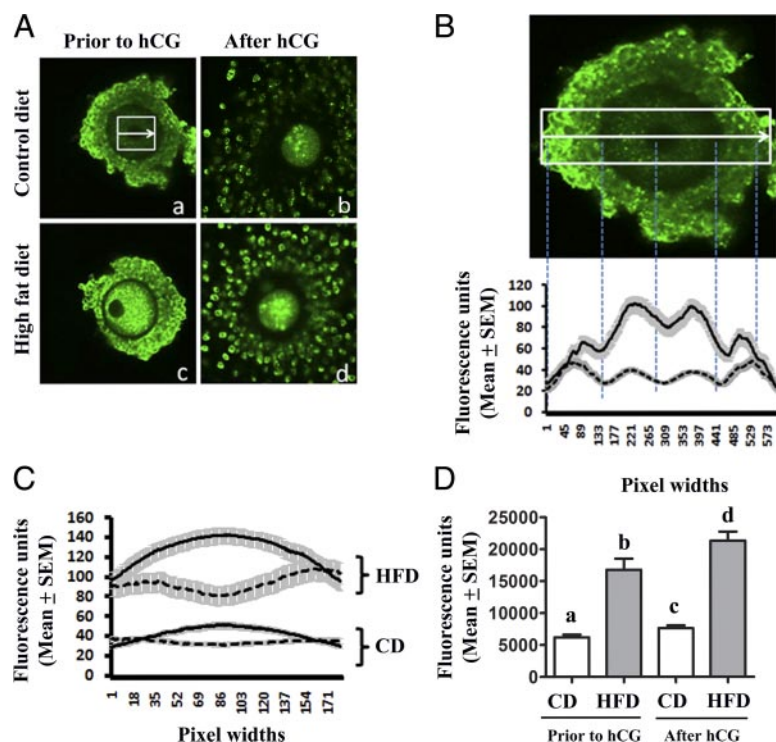


**FIG. 1.** High-fat diet increases lipid content in the COC. COCs were collected from mice fed a high-fat diet (HFD) or control diet (CD) for 4 weeks and stained for neutral lipids with BODIPY 493/503. Immature unexpanded COCs were isolated from preovulatory follicles 44 h after eCG administration (before hCG), and mature COCs were obtained from oviducts 13 h post hCG. A, COCs from HFD-fed mice (c and d) showed markedly higher levels of lipid than COCs from mice fed control diet (a and b) both before and after ovulation. B, Lipid levels in immature COCs were assessed by placing a box across the entire COC image and measuring pixel intensity. Lipid levels were higher in both cumulus cells and oocytes of mice fed high-fat diet [solid line = mean  $\pm$  SEM (shaded);  $n = 32$  COCs from 6 mice] compared with those fed control diet [dashed line = mean  $\pm$  SEM (shaded);  $n = 42$  COCs from 6 mice]; significantly increased from position 59 to 578 across the complex ( $P < 0.0001$ ; two-way ANOVA, Bonferroni post hoc test). C, Oocyte lipid levels were assessed by placing a box over the oocyte (as in A) and measuring pixel intensity. Lipid levels were dramatically higher ( $P < 0.0001$ ; two-way ANOVA, Bonferroni post hoc test) in both preovulatory [dashed lines = mean  $\pm$  SEM (shaded)] and ovulated [solid lines = mean  $\pm$  SEM (shaded)] oocytes from mice fed high-fat diet ( $n = 35$  or 45 COCs from 6 mice per diet) compared with oocytes from mice fed control diet ( $n = 39$  or 42 COCs from 6 mice of each diet). D, Total oocyte lipid content per area was calculated as the sum total of fluorescence in the boxed region of each oocyte. Different letters indicate significant differences by two-way ANOVA, Bonferroni post hoc test.

Proteinase K was added (50  $\mu$ l of 10 mg/ml solution) and samples incubated overnight at room temperature. Protein was precipitated by the dropwise addition of 200  $\mu$ l of 4 M NaCl and samples centrifuged at 10,000  $\times g$  for 30 min at 4 C. The supernatant was extracted with phenol:chloroform:isoamyl alcohol (25:24:1) and DNA precipitated with EtOH (70% v/v) and resuspended in Tris-EDTA buffer [10 mM Tris Base, 1 mM EDTA, 0.05% Tween 20 (pH 9.0)] containing 70  $\mu$ g/ml RNase. DNA concentration and purity were quantified using a Nanodrop ND-1000 Spectrophotometer (Biolab), and 8  $\mu$ g of each sample were run on 3% agarose gels in TBE buffer [45 mM Tris, 45 mM boric acid, 1 mM EDTA (pH 8.0)]. Bands were detected by ethidium bromide staining and intensity of each band quantified using ImageJ software (<http://rsb.info.nih.gov/ij/>).

### TUNEL assay

Ovaries were fixed in 4% paraformaldehyde/PBS at 4 C overnight and embedded in paraffin. Sections were cut serially at 5

$\mu$ m thickness and every fifth section collected on a microscope slide, to a total of 15 sections for each ovary. TUNEL assay was performed using TUNEL Universal Apoptosis Detection Kit (GenScript) as per the manufacturer's instructions, with DAPI to counterstain nuclei. Fluorescent images were acquired on Olympus BX51 microscope and TUNEL-positive and DAPI-stained cells quantified using ImageJ software (<http://rsb.info.nih.gov/ij/>) to minimize subjectivity in manual cell counting. Apoptotic index was calculated as TUNEL-positive cells per thousand cumulus or granulosa cells.

### Assessment of ovulation and *in vivo* fertilization rate

Mice were injected i.p. at 1400 with 5 I.U. per 12 g body weight of eCG, followed 44 h later by 5 I.U. per 12 g body weight of hCG and caging with a male. Ovulated oocytes were isolated from the oviduct at 1300 the following day and maintained in G1 media (23). Fertilization rate, as indicated by first cleavage division, was assessed 19 h later.

### Analyses of human follicular fluid and granulosa cells

The study group was recruited from women seeking assisted reproduction at a private clinic in South Australia (Repromed). Ethics approval was obtained from the Women's and Children's Hospital, Adelaide, South Australia. Patients were allocated to one of three groups based on body mass index (BMI = weight/height): moderate (BMI = 20–24.9 kg/m<sup>2</sup>), overweight (BMI = 25–29.9 kg/m<sup>2</sup>), and obese (BMI  $\geq$  30 kg/m<sup>2</sup>). Additional information about this cohort has been previously published (24). Briefly, all patients were administered daily recombinant FSH (150–300 IU) from the start of their menstrual cycle

for 8–10 d until a minimum of three follicles of more than 18 mm diameter was observed by transvaginal ultrasound scan. GnRH antagonist (Orgalutron) was used from d 6 of the cycle to block ovulation. Women were then administered hCG (Ovidrel 250  $\mu$ g), and transvaginal follicular aspiration was performed 36 h after hCG administration. Blood-free follicular aspirates were centrifuged at 4000 rpm for 10 min and the follicle fluid removed and stored at  $-80^{\circ}\text{C}$ . Follicular fluid Ca<sup>2+</sup> levels were determined by Roche Hitachi 912 Chemistry Analyzer as per manufacturer's instructions, and using quality controls QCS1 and 2 (Bio-Rad).

Granulosa cells were pooled from follicular aspirates of each patient and total RNA isolated using a modified Tri Reagent (Sigma-Aldrich, St. Louis, MO) protocol, including an overnight precipitation step at  $-20^{\circ}\text{C}$ , and resuspension of the final pellet in 25  $\mu$ l ultrapure water. All samples were deoxyribonuclease-treated using Ambion DNA-free (Applied Biosystems, Foster City, CA). RNA quantification, RT, and real-time PCR were performed as above.



## Statistical analysis

All measures are reported as mean  $\pm$  SEM. Statistical significance was determined as indicated; by *t* test, two-way ANOVA with Bonferroni post hoc tests, Fishers Exact Test, Student-Newman-Keuls, or Spearman correlation test, as appropriate, using Graph Pad Prism version 5.01 for Windows (GraphPad Software Inc., San Diego, CA). A *P* value of  $<0.05$  was considered statistically significant.

## Results

### Effect of high-fat diet on oocyte lipid content

To determine whether dietary fat consumption influences lipid content of the COC, lipid droplet abundance and localization were measured using BODIPY 493/503 stain. Oocytes from mice fed high-fat diet showed visibly higher levels of lipid than those from mice fed control diet (Fig. 1A) both before and after ovulation. Quantification of lipid levels showed that in immature unexpanded COCs lipid content was significantly higher in both cumulus cells and oocytes of mice fed high-fat diet compared with those fed control diet (Fig. 1B). Analysis of lipid distribution in oocytes showed that those from mice fed control diet had low levels of lipid which re-localized to the center of the oocyte in response to ovulatory hCG (Fig. 1C). Mice fed high-fat diet had dramatically higher levels of lipid within oocytes of unexpanded preovulatory COCs which similarly relocalized to the center in response to ovulatory hCG (Fig. 1C). Expressed as total lipid, oocytes from mice fed high-fat diet have markedly increased lipid content, both before and after ovulation, compared with oocytes of mice fed control diet (Fig. 1D).

### Effect of high-fat diet on indices of lipotoxicity in ovarian follicular cells and oocytes

The clear increase in lipid content in COCs of mice fed high-fat diet led to investigations of whether this excessive intracellular lipid content is associated with the activation of lipotoxicity pathways, namely activation of ER stress, altered mitochondrial membrane potential, or increased apoptosis. The presence of ER stress was determined by measuring the expression of well-characterized ER stress marker genes (ATF4, GRP78, CHOP10, and Hsp70) in granulosa cells and COCs isolated from preovulatory follicles of eCG-treated mice. ATF4 is a transcription factor up-regulated during ER stress that induces an additional transcriptional regulator CHOP10 as well as the chaperone GRP78 as part of the unfolded protein response. GRP78, also known as Hspa5, and Hsp70 are both heat shock proteins involved in maintaining proper protein folding and assembly in the ER. There were significantly higher levels of ATF4 and GRP78 expression in COCs from high-fat diet-fed mice relative to the levels of control

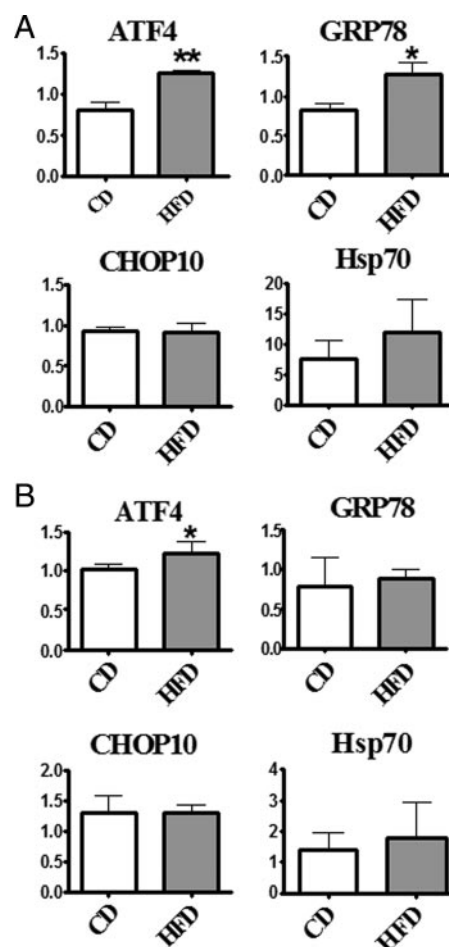


**FIG. 2.** ER stress genes are induced in COCs and granulosa cells by high-fat diet. mRNA expression of ER stress marker genes in COCs (A) and granulosa cells (B) from mice fed control diet (CD) or high-fat diet (HFD). COCs from mice fed HFD expressed higher levels of both ATF4 and GRP78. Granulosa cells from mice fed HFD expressed higher levels of ATF4. Values are mean  $\pm$  SEM expressed as fold change compared with calibrator sample; *n* = 3 pools of cells per diet, each isolated from 4 mice. \*\*, *P* < 0.01; \*, *P* < 0.05; by *t* test.

diet-fed mice, but no significant difference in expression of CHOP10 or Hsp70 (Fig. 2A). ATF4 expression was also increased in granulosa cells of mice fed high-fat diet (Fig. 2B).

Mitochondrial membrane potential (MMP) of oocytes was determined by staining with the inner membrane potential dye JC-1. In oocytes from control diet-fed mice red punctuate fluorescence indicating high MMP mitochondria was localized to the pericortical region, and green fluorescence indicating low MMP mitochondria was localized to the deeper cytoplasm (Fig. 3A: a and b) consistent with previous reports (25). In oocytes from high-fat diet-fed mice, red fluorescence intensity was reduced (Fig. 3A: c and d), while green fluorescence appeared increased. Mitochondrial damage initially manifests as a decrease in the mitochondrial membrane potential, with reductions in MMP status, determined by the ratio of red to green fluorescence, considered a hallmark of mitochondrial dam-

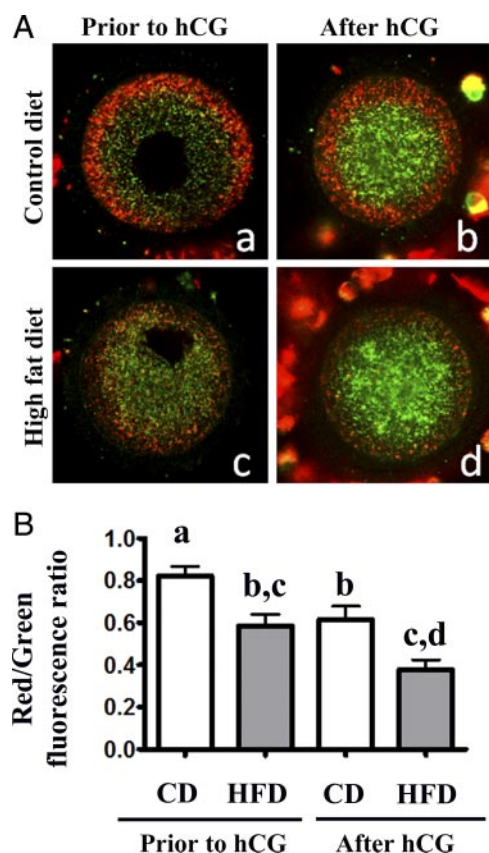


**FIG. 3.** Oocyte mitochondrial membrane potential is reduced in mice fed high-fat diet. Mitochondrial membrane potential was assessed by JC-1 staining (A) in immature oocytes from eCG-treated mice (a and c) and mature oocytes from eCG, hCG 13 h-treated mice (b and d) fed control diet (CD) or high-fat diet (HFD). The ratio of red/green fluorescence was quantified (B) as an indicator of mitochondrial damage. Data are presented as mean  $\pm$  SEM,  $n = 30$  oocytes from three mice per diet. Different letters indicate significant differences by two-way ANOVA, Bonferroni post test.

age (26, 27). The mean ratio of red/green fluorescence intensity of oocytes from control diet-fed mice was decreased in mature ovulated oocytes compared with preovulatory oocytes (Fig. 3B). In mice fed high-fat diet, the mean ratio of red/green fluorescence was significantly reduced in both immature preovulatory and mature ovulated oocytes compared with oocytes from control diet mice (Fig. 3B), demonstrating that oocytes from high-fat diet-fed mice have reduced MMP that is indicative of mitochondrial damage.

The incidence of apoptosis in granulosa cells and COCs of preovulatory follicles was investigated. DNA laddering assay showed that granulosa cells from high-fat diet-fed mice have greater 180-bp and 360-bp band intensities compared with cells from control diet-fed mice (Fig. 4, A and B), indicating increased DNA fragmentation. TUNEL assay on ovarian sections confirmed this result by demonstrating more TUNEL-positive cells within the ovarian follicles of mice fed high-fat diet compared with control diet (Fig. 4, C and D). The apoptotic index reached

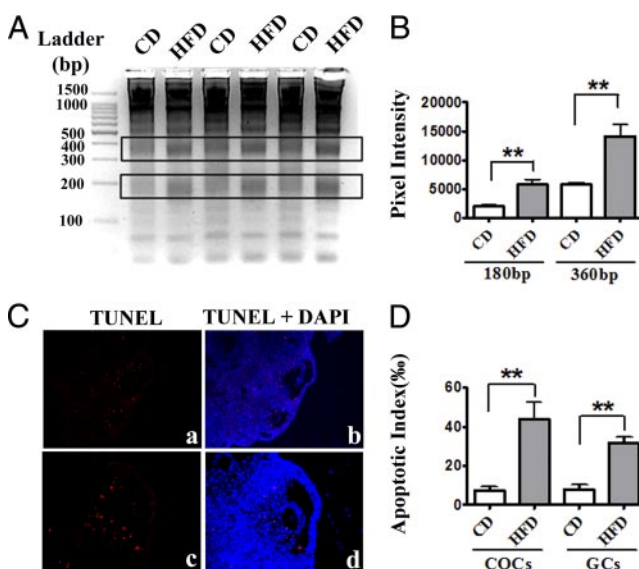


**FIG. 4.** High-fat diet increases apoptosis in cumulus and granulosa cells. A, DNA ladder analysis of granulosa cells from mice fed control diet (CD) or high-fat diet (HFD). B, Quantification of 180-bp and 360-bp band intensities, boxed in A. Data are presented as mean  $\pm$  SEM;  $n = 3$  pools of cells per diet, each isolated from 10 mice. \*\*,  $P < 0.001$ ,  $t$  test. C, Representative TUNEL-positive (red) and total cell (DAPI, blue) stained ovary sections showing multiple follicles (a and b) and a single follicle at higher power (c and d). Left panel is red-channel only of right panel. D, Apoptotic indices of the cumulus (COCs) and granulosa cells (GCs) from CD- and HFD-fed mice. Data are presented as mean  $\pm$  SEM,  $n = 4$  mice per diet. \*\*,  $P < 0.01$ ,  $t$  test.

44.03% in cumulus cells and 31.83% in granulosa cells from high-fat diet-fed mice compared with 7.6% and 7.65%, respectively, in control diet-fed mice.

#### Effects of high-fat diet on expression of FSH/LH target genes, ovulation, and fertilization

To determine whether mice fed high-fat diet exhibit altered ovarian responsiveness to gonadotropins, we analyzed granulosa cell expression of FSH-receptor and LH-receptor, and Cyp19a1 (P450 aromatase) and Cyp11a1 (P450 cholesterol side-chain cleavage), FSH- and LH-responsive genes, respectively. There were no significant differences, in either eCG- or eCG + hCG-treated mice, in expression levels of FSH-Receptor, Cyp11a1, LH-Receptor, or Cyp19a1 in granulosa cells from mice fed high-fat diet relative to levels of control diet-fed mice (Fig. 5).

To determine the impact on ovulation and fertilization, female mice fed control diet or high-fat diet were treated with gonadotropins and caged with a male mouse. All control diet-fed mice ovulated ( $n = 22$ ); however, in several high-fat diet-fed mice (6 of 23) zero oocytes were present in both oviducts, resulting in a 26% incidence of anovulation ( $P = 0.02$  compared with control diet; Fisher's Exact Test). The average number of oocytes ovulated, however, was not different between the two groups: mice fed control diet ovulated a mean of  $15.9 \pm 4.7$  oocytes,

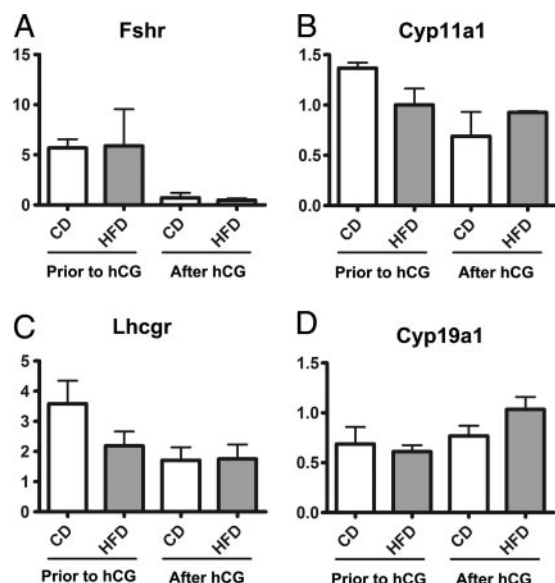


**FIG. 5.** Normal expression of FSH/LH target genes in granulosa cells of mice fed high-fat diet. Expression of FSH-Receptor (A), Cyp11a1 (B), LH-Receptor (C), and Cyp19a1 (D) was measured in granulosa cells from eCG (before hCG) or eCG + hCG 13 h-treated mice fed control diet (CD) or high-fat diet (HFD). There were no significant differences by *t* test in cells from mice fed HFD compared with those fed CD, at either time point. Values are mean  $\pm$  SEM expressed as fold change compared with calibrator sample; *n* = 2 pools of cells per diet, each isolated from four mice treated with eCG; *n* = 3 pools of cells per diet, each isolated from 4 mice treated with eCG, hCG.

with a range of 9 to 36 per female. Mice fed high-fat diet ovulated a mean of  $10.4 \pm 2.3$  oocytes, with a range of 0 to 26 per female. The ovulated oocytes from high-fat diet-fed mice were morphologically indistinguishable from those of control diet-fed mice; however, only 52.6% of oocytes from high-fat diet-fed mice were fertilized compared with 69.6% of oocytes from control-fed mice ( $P = 0.0003$ , Fisher's Exact Test). The fertilized oocytes from both control diet and high-fat diet mice exhibited similar developmental dynamics and formed blastocysts that were morphologically identical (data not shown). Thus, although mice fed high fat appear capable of responding to eCG and hCG treatment, anovulation occurs in a significant proportion and fertilization rate is compromised.

### Measures of ER stress in ovarian follicles of obese women

Indicators of lipotoxicity were analyzed where possible in follicular fluid or ovarian cells of women of varying BMI to determine whether lipotoxicity pathways may be activated in the human ovary in response to obesity. Disrupted  $\text{Ca}^{2+}$  homeostasis is a prominent feature of ER stress, and  $\text{Ca}^{2+}$  can be liberated from dying cells; thus  $\text{Ca}^{2+}$  levels in follicular fluid were determined in women of varying BMI. Follicular fluid  $\text{Ca}^{2+}$  levels were positively correlated with increasing BMI (Fig. 6A). Further,  $\text{Ca}^{2+}$  levels were positively correlated with follicular fluid triglyceride, free

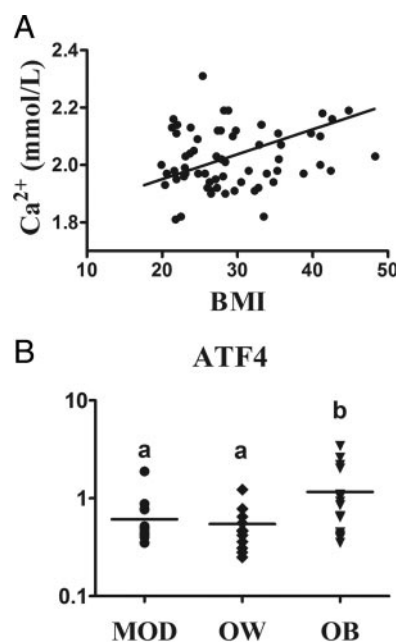


**FIG. 6.** Lipotoxicity pathways may be activated in ovarian follicles of obese women. A, Follicle fluid  $[\text{Ca}^{2+}]$  levels increase with increasing body mass index (BMI;  $\text{kg}/\text{m}^2$ );  $P = 0.01$  by Spearman correlation test, *n* = 64. B, Expression of ER stress marker gene ATF4 is significantly higher in granulosa cells from obese women (OB; *n* = 15) than moderate (MOD; *n* = 15) and overweight women (OW; *n* = 12). Expression levels were log10 transformed to normalize and expressed as fold change compared with a calibrator sample. Horizontal lines represent the mean of each group. Different letters indicate differences in groups by Student–Newman–Keuls.  $P < 0.05$ .

fatty acids, and glucose ( $P = 0.002$ ,  $P = 0.003$ , and  $P = 0.0007$ , respectively, Spearman correlation) but not other follicular fluid constituents (such as steroids), suggesting an association of ER stress with the increased follicular fluid glucose and dyslipidemia that occurs in obese women (24). Secondly, the ER stress marker gene ATF4, which was elevated in mouse granulosa cells in response to high-fat diet, was analyzed in human granulosa cells. ATF4 expression was significantly increased in granulosa cells from obese women compared with granulosa cells of moderate or overweight women (Fig. 6B), suggesting that ER stress pathways are activated in granulosa cells of obese women.

### Discussion

This study identifies functional cellular defects that arise in the ovary and oocyte in response to obesity. Specifically, we have found that a high-fat diet causes increased lipid accumulation, induction of ER stress pathway genes, altered mitochondrial membrane potential, and increased incidence of apoptosis in ovarian cells—responses that are characteristic biomarkers of lipotoxicity (12, 14, 28). Further we have preliminary evidence (Fig. 6) that similar responses are occurring in the ovaries of women who are obese.



We have previously found that triglyceride levels are increased in follicular fluid of obese women (24), but the current results are the first to directly demonstrate that high-fat diet dramatically increases the lipid content of immature and mature oocytes, as well as their surrounding cumulus cells. Whether the observed increase in intracellular lipid is due to diffusion from serum or follicular fluid, or *de novo* lipogenesis in response to elevated glucose levels, is under investigation; however, lipid accumulation in cells other than adipocytes is generally considered the initiating event in lipotoxicity pathways (28).

The induction of ER stress, namely up-regulation of the UPR signaling pathway, is a classic response to lipotoxicity (12, 14). We examined four components of this response and found that ATF4 and GRP78 were specifically up-regulated in granulosa cells and COCs of mice fed high-fat diet, and that ATF4 was up-regulated in granulosa cells of obese women. ATF4, a transcription factor induced downstream of PRKR-like ER kinase (PERK), induces expression of genes involved in amino acid metabolism, the antioxidant response, and apoptosis, including the proapoptotic factor CHOP. Thus it was somewhat surprising that CHOP mRNA, like ATF4, was not increased by high-fat diet; however, long-term exposure to mild stress can lead to adaptations in CHOP expression (29). In contrast GRP78 (also known as BiP) is a prosurvival factor induced during UPR that remains elevated even in response to chronic stress (29). It is interesting that GRP78 was induced by high-fat diet specifically in COCs suggesting that the oocyte is undergoing a distinct UPR response or that its presence influences the stress response of adjacent cumulus cells. The induction of chaperones is an additional key reaction to the presence of ER stress and unfolded proteins, and we chose Hsp70 as an example to investigate; however its levels appeared more variable and were not significantly up-regulated by high-fat diet. In addition, calcium levels, which are dysregulated by ER stress and can be indicative of cell death by apoptosis, were elevated in the follicular fluid of obese women. We speculate that the increase in calcium is derived from ovarian cells because two previous reports have shown that calcium levels are not increased in the serum of obese women (30, 31). It is also relevant that ER stress, via activation of the CREBH transcription factor, induces aspects of the acute phase response, particularly C-reactive protein (32), which we have previously reported is positively correlated with BMI in the follicular fluid of women (24). Cumulatively, these observations strongly suggest that ER stress pathways are activated in the ovarian cells of obese women.

Alterations in mitochondrial membrane potential are another classical response to cellular stress including lipotoxicity (10, 12, 33), and one that is tightly linked to

stress responses in the ER. Mitochondrial membrane potential was significantly reduced by high-fat diet in both immature and mature oocytes, an alteration that is known to have significant consequences on oocyte developmental competence (34–37) as mitochondria play vital roles in metabolism and the energy-dependent mechanisms that generate ATP and maintain cellular homeostasis in the oocyte and early embryo. Loss of membrane potential also leads to uncoupling of oxidative phosphorylation, oxygen radical generation, release of cytochrome c, and activation of caspases, the initiators of DNA fragmentation (38, 39). Whether changes in mitochondrial membrane potential influence the induction of ER stress pathways or *vice versa* is not known (40, 41); however, both cellular responses are known to culminate in apoptosis (41). Consistent with this, our results show that apoptotic rate increased in cumulus cells and granulosa cells of mice fed high-fat diet compared with those fed control diet.

Cumulatively, the present demonstration of elevated lipid content and decreased mitochondrial membrane potential in oocytes of mice fed high-fat diet implicates these mechanisms of lipotoxicity as likely contributors to the reduced fertilization rates in these mice and the reduced natural conception rates seen in obese women.

## Acknowledgments

We acknowledge the expert technical assistance of Lisa K. Akison, Brenton D. Bennet, Dr. Miles Deblasio (analysis of serum metabolites), and Prof. David Kennaway (insulin assay).

Address all correspondence and requests for reprints to: Rebecca Robker, School of Pediatrics and Reproductive Health, University of Adelaide, Adelaide, South Australia 5005, Australia. E-mail: Rebecca.robker@adelaide.edu.au.

This work was supported by the National Health and Medical Research Council (to M.L., R.J.N., R.L.R.) and the Channel 7 Children's Research Fund (to L.L.W., R.L.R.).

Disclosure Summary: The authors have nothing to declare.

## References

1. Rich-Edwards JW, Spiegelman D, Garland M, Hertzmark E, Hunter DJ, Colditz GA, Willett WC, Wand H, Manson JE 2002 Physical activity, body mass index, and ovulatory disorder infertility. *Epidemiology* 13:184–190
2. Grodstein F, Goldman MB, Cramer DW 1994 Body mass index and ovulatory infertility. *Epidemiology* 5:247–250
3. Mulders AG, Laven JS, Eijkemans MJ, Hughes EG, Fauser BC 2003 Patient predictors for outcome of gonadotrophin ovulation induction in women with normogonadotrophic anovulatory infertility: a meta-analysis. *Hum Reprod Update* 9:429–449
4. Jensen TK, Scheike T, Keiding N, Schaumburg I, Grandjean P 1999 Fecundability in relation to body mass and menstrual cycle patterns. *Epidemiology* 10:422–428

5. Ramlau-Hansen CH, Thulstrup AM, Nohr EA, Bonde JP, Sørensen TI, Olsen J 2007 Subfecundity in overweight and obese couples. *Hum Reprod* 22:1634–1637
6. Gesink Law DC, Macle hose RF, Longnecker MP 2007 Obesity and time to pregnancy. *Hum Reprod* 22:414–420
7. van der Steeg JW, Steures P, Eijkemans MJ, Habbema JD, Hompes PG, Burggraaff JM, Oosterhuis GJ, Bossuyt PM, van der Veen F, Mol BW 2008 Obesity affects spontaneous pregnancy chances in subfertile, ovulatory women. *Hum Reprod* 23:324–328
8. Zaadstra BM, Seidell JC, Van Noord PA, te Velde ER, Habbema JD, Vrieswijk B, Karbaat J 1993 Fat and female fecundity: prospective study of effect of body fat distribution on conception rates. *BMJ* 306:484–487
9. Schaffer JE 2003 Lipotoxicity: when tissues overeat. *Curr Opin Lipidol* 14:281–287
10. Li Z, Berk M, McIntyre TM, Gores GJ, Feldstein AE 2008 The lysosomal-mitochondrial axis in free fatty acid-induced hepatic lipotoxicity. *Hepatology* 47:1495–1503
11. Ilieva EV, Ayala V, Jové M, Dalfó E, Cabellos D, Povedano M, Bellmunt MJ, Ferrer I, Pamplona R, Portero-Otín M 2007 Oxidative and endoplasmic reticulum stress interplay in sporadic amyotrophic lateral sclerosis. *Brain* 130:3111–3123
12. Malhi H, Gores GJ 2008 Molecular mechanisms of lipotoxicity in nonalcoholic fatty liver disease. *Semin Liver Dis* 28:360–369
13. Diakogiannaki E, Welters HJ, Morgan NG 2008 Differential regulation of the endoplasmic reticulum stress response in pancreatic beta-cells exposed to long-chain saturated and monounsaturated fatty acids. *J Endocrinol* 197:553–563
14. Borradaile NM, Han X, Harp JD, Gale SE, Ory DS, Schaffer JE 2006 Disruption of endoplasmic reticulum structure and integrity in lipotoxic cell death. *J Lipid Res* 47:2726–2737
15. Rutkowski DT, Kaufman RJ 2004 A trip to the ER: coping with stress. *Trends Cell Biol* 14:20–28
16. Kaufman RJ 1999 Stress signaling from the lumen of the endoplasmic reticulum: coordination of gene transcriptional and translational controls. *Genes Dev* 13:1211–1233
17. Hamada Y, Fujii H, Fukagawa M 2009 Role of oxidative stress in diabetic bone disorder. *Bone* 45 (Suppl 1):S35–S38
18. Li N, Frigerio F, Maechler P 2008 The sensitivity of pancreatic beta-cells to mitochondrial injuries triggered by lipotoxicity and oxidative stress. *Biochem Soc Trans* 36:930–934
19. Schrauwen P, Hesselink MK 2004 Oxidative capacity, lipotoxicity, and mitochondrial damage in type 2 diabetes. *Diabetes* 53:1412–1417
20. Ozcan U, Cao Q, Yilmaz E, Lee AH, Iwakoshi NN, Ozdelen E, Tuncman G, Görgün C, Glimcher LH, Hotamisligil GS 2004 Endoplasmic reticulum stress links obesity, insulin action, and type 2 diabetes. *Science* 306:457–461
21. Ozcan L, Ergin AS, Lu A, Chung J, Sarkar S, Nie D, Myers Jr MG, Ozcan U 2009 Endoplasmic reticulum stress plays a central role in development of leptin resistance. *Cell Metab* 9:35–51
22. Minge CE, Bennett BD, Norman RJ, Robker RL 2008 Peroxisome proliferator-activated receptor-gamma agonist rosiglitazone reverses the adverse effects of diet-induced obesity on oocyte quality. *Endocrinology* 149:2646–2656
23. Gardner DK, Lane M, Watson AJ 2004 A laboratory guide to the mammalian embryo. New York: Oxford University Press; 43–44
24. Robker RL, Akison LK, Bennett BD, Thrupp PN, Chura LR, Russell DL, Lane M, Norman RJ 2009 Obese women exhibit differences in ovarian metabolites, hormones, and gene expression compared with moderate-weight women. *J Clin Endocrinol Metab* 94:1533–1540
25. Van Blerkom J, Davis P, Mathwig V, Alexander S 2002 Domains of high-polarized and low-polarized mitochondria may occur in mouse and human oocytes and early embryos. *Hum Reprod* 17:393–406
26. Vayssier-Taussat M, Kreps SE, Adrie C, Dall'Ava J, Christiani D, Polla BS 2002 Mitochondrial membrane potential: a novel biomarker of oxidative environmental stress. *Environ Health Perspect* 110:301–305
27. Savitha S, Panneerselvam C 2006 Mitochondrial membrane damage during aging process in rat heart: potential efficacy of L-carnitine and DL alpha lipoic acid. *Mech Ageing Dev* 127:349–355
28. Szendroedi J, Roden M 2009 Ectopic lipids and organ function. *Curr Opin Lipidol* 20:50–56
29. Rutkowski DT, Arnold SM, Miller CN, Wu J, Li J, Gunnison KM, Mori K, Sadighi Akha AA, Raden D, Kaufman RJ 2006 Adaptation to ER stress is mediated by differential stabilities of pro-survival and pro-apoptotic mRNAs and proteins. *PLoS Biol* 4:e374
30. Mahmoudi T, Gourabi H, Ashrafi M, Yazdi RS, Ezabadi Z 2010 Calcitropic hormones, insulin resistance, and the polycystic ovary syndrome. *Fertil Steril* 93:1208–1214
31. Yildizhan R, Kurdoglu M, Adali E, Kulusari A, Yildizhan B, Sahin HG, Kamaci M 2009 Serum 25-hydroxyvitamin D concentrations in obese and non-obese women with polycystic ovary syndrome. *Arch Gynecol Obstet* 280:559–563
32. Zhang K, Kaufman RJ 2006 Protein folding in the endoplasmic reticulum and the unfolded protein response. *Handb Exp Pharmacol* 172:69–91
33. Schrauwen P, Schrauwen-Hinderling V, Hoeks J, Hesselink MK 2010 Mitochondrial dysfunction and lipotoxicity. *Biochim Biophys Acta* 1801:266–271
34. Cummins JM 2004 The role of mitochondria in the establishment of oocyte functional competence. *Eur J Obstet Gynecol Reprod Biol* 115 (Suppl 1):S23–S29
35. Fujii W, Funahashi H 2009 Exogenous adenosine reduces the mitochondrial membrane potential of murine oocytes during the latter half of in vitro maturation and pronuclear formation following chemical activation. *J Reprod Dev* 55:187–193
36. Mitchell M, Schulz SL, Armstrong DT, Lane M 2009 Metabolic and mitochondrial dysfunction in early mouse embryos following maternal dietary protein intervention. *Biol Reprod* 80:622–630
37. Kanaya H, Hashimoto S, Teramura T, Morimoto Y, Matsumoto K, Saeki K, Iritani A, Hosoi Y 2007 Mitochondrial dysfunction of in vitro grown rabbit oocytes results in preimplantation embryo arrest after activation. *J Reprod Dev* 53:631–637
38. Susin SA, Lorenzo HK, Zamzami N, Marzo I, Brenner C, Larochette N, Prévost MC, Alzari PM, Kroemer G 1999 Mitochondrial release of caspase-2 and -9 during the apoptotic process. *J Exp Med* 189:381–394
39. Backway KL, McCulloch EA, Chow S, Hedley DW 1997 Relationships between the mitochondrial permeability transition and oxidative stress during ara-C toxicity. *Cancer Res* 57:2446–2451
40. Lee MJ, Kee KH, Suh CH, Lim SC, Oh SH 2009 Capsaicin-induced apoptosis is regulated by endoplasmic reticulum stress- and calpain-mediated mitochondrial cell death pathways. *Toxicology* 264:205–214
41. Arduíno DM, Esteves AR, Cardoso SM, Oliveira CR 2009 Endoplasmic reticulum and mitochondria interplay mediates apoptotic cell death: relevance to Parkinson's disease. *Neurochem Int* 55:341–348